

Early proliferation of avicularia in the Cretaceous cheilostome bryozoan *Wilbertopora*: a diversification event guided by ecological exploration

Sarah Leventhal*

Department of Geological Sciences, University of Colorado Museum of Natural History University of Colorado, Boulder, CO, USA

ORCID ID: 0000-0002-6537-1553

Kayli Stowe

Department of Geological Sciences, University of Colorado Museum of Natural History University of Colorado, Boulder, CO, USA

Carl Simpson

Department of Geological Sciences, University of Colorado Museum of Natural History University of Colorado, Boulder, CO, USA

ORCID ID: 0000-0003-0719-4437

ABSTRACT: Cheilostome bryozoans are a diverse clade of colonial animals that first appeared during the Jurassic period. For the first 100 Myr of their existence, colonies of cheilostomes were monomorphic, composed entirely of autozooids. Divergent body types, termed avicularia, first appeared in colonies in the early Cretaceous period, in the genus *Wilbertopora*. Over the course of the Cretaceous, *Wilbertopora* diversified into 27 species, spanning the early Albian through Maastrichtian stages. In this study, we quantify autozooid and avicularia shape and size to evaluate how the morphological disparity of zooid types in colonies changes over the course of *Wilbertopora*'s diversification. We find that taxonomic diversity and morphological disparity are largely decoupled, with disparity outpacing diversity for much of *Wilbertopora*'s evolutionary history. Increases in disparity are primarily driven by evolution of avicularian morphology, indicating that *Wilbertopora*'s avicularia may have served an array of purposes in different lineages.

1 INTRODUCTION

Extant cheilostome bryozoans possess a wide range of polymorphs that have proved to be an important innovation for the success of the clade (Jablonski *et al.* 1997; Taylor 2020). Polymorphs, in the form of avicularia, first evolved in the late Albian cheilostome *Wilbertopora* (Cheetham 1954; Ostrovsky *et al.* 2008) (Figure 1), which underwent a brief but explosive diversification event until the end of the Maastrichtian (Cheetham *et al.* 2006; Taylor 2020). Over the course of this period, *Wilbertopora* diversified into a total of 27 species.

While *Wilbertopora* is the first genus of cheilostomes to have avicularia, the evolution of its avicularian morphology has never been subject to quantitative study. Here we evaluate the taxonomic diversification of *Wilbertopora* (Cheetham 1954; Ostrovsky *et al.* 2008; Cheetham *et al.* 2006) and quantify the morphological disparity of zooid types in colonies over the course of this diversification.

We present an analysis of the trajectory of morphological disparity and taxonomic diversity in 25 of the 27 species of *Wilbertopora* from the genus's first appearance in the Albian to its last appearance in Maastrichtian. To better understand the evolving morphologies of different zooid types in *Wilbertopora*, we also directly compare disparity of autozooids and avicularia over time.

2 METHODS

2.1 Data aggregation and analytical methodology

To estimate of the number of *Wilbertopora* species that existed over the genus' life span, we compiled publications containing references to the genus from Bock (2020). Then, we filtered out publications that mention the genus but do not describe a specific occurrence of its species. This process left us with publications detailing 27 distinct species. Fossils of distinct *Wilbertopora* species have been found in the Albian, Cenomanian, Campanian, and Maastrichtian stages of Texas (Cheetham *et al.* 2006); the Campanian and Maastrichtian of

*Corresponding Author: sarah.leventhal@colorado.edu

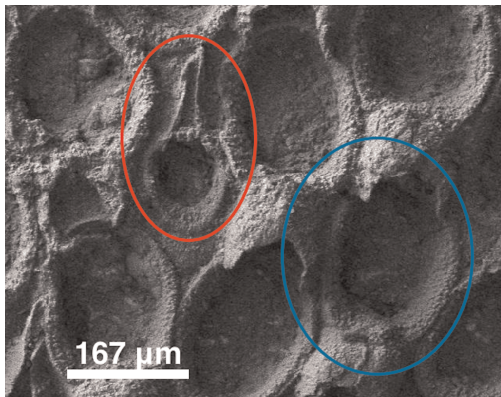


Figure 1. Photograph of *Wilbertopora acuminata*, a species of *Wilbertopora* from the late Albian/early Cenomanian. Avicularium is circled in red, and autozooid is circled in blue. Specimen is from NHM London, NHM PI BZ 1479.

southern California, Baja California (Taylor 2008), Kazakhstan (Koromyslova *et al.* 2018), and the southeastern United States (Taylor & McKinney 2006); the Cenomanian, Turonian, and Campanian of England (Smith and Batten 2002; Taylor & Martha 2017); the late Cretaceous of the United Arab Emirates (Di Martino & Taylor 2013); the mid-late Cretaceous of western and central Europe (Martha & Taylor 2016; Voigt 1981); the Cenomanian of India (Guha 1989; Taylor & Badve 1994); and the Maastrichtian of Madagascar (Di Martino *et al.* 2018).

We recorded occurrence information from each of these publications to get an estimate of first and last appearances for each species. We removed two species for which we could not access adequate SEM images or measurement information in monographs: *Wilbertopora stoliczki* (Guha 1989), and *Wilbertopora? bohemica* from the Czech Republic (Žitt *et al.* 2006). We therefore consider 25 species of *Wilbertopora* in our analysis.

To assess the macroevolutionary patterns in early avicularia evolution, we use Jablonski's (2017) diversity-disparity analysis. This type of analysis allows for us to make broad ecological interpretations about patterns of morphological disparity and taxonomic diversity (Figure 2). There are three general diversification patterns observable using this type of analysis (Jablonski 2017). Trajectories that fall below the 1:1 line (Type 3) exhibit ecological exploitation, where diversification occurs without major increase in disparity. The conservation of morphology through taxonomic diversification suggests that niche exploitation guides diversification. Conversely, trajectories falling above the 1:1 line (Type 1) exhibit what we term ecological exploration. In these types of diversification events, increases in morphological disparity outpace

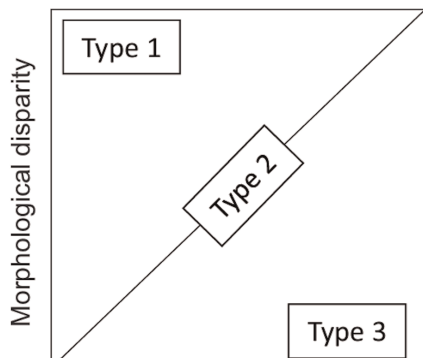


Figure 2. Diversity-disparity analytical framework applied in this study as adapted from Jablonski (2017, fig. 4). There are three main patterns of diversification. Type 1 refers to diversification events where increases in disparity outpace increases in taxonomic diversity, or “ecological exploration.” Type 2 refers to events with concordant increases of disparity and taxonomic diversity, which follows a line with a slope of 1. Type 3 refers to events with increases in taxonomic diversity that outpace increases in disparity, or “ecological exploitation.”

increases in taxonomic diversity. This pattern would suggest that different lineages of the subject taxon may be pursuing different ecological niches or experiencing genetic drift. Trajectories tracking with the 1:1 line (Type 2) follow the expected pattern of concordant increases in disparity and diversity (Jablonski 2017).

2.2 Estimating diversity

To assess diversity over time, we first compiled all occurrence information from monographs describing the 25 *Wilbertopora* species. Due to the incompleteness of the fossil record, we generated a tip-dated phylogeny to better estimate fossil ranges for each species. Since this is one of the few morphology-based phylogenies of more than a handful of bryozoan species, we first compiled a list of applicable characters based on previous smaller phylogenetic studies (Cheetham *et al.* 2006), but this did not provide us with enough characters to construct a phylogeny for our 25 species. Only 15 of the 20 significant characters included in Cheetham *et al.*'s (2006) analysis could be determined from monographs or available specimen SEMs. Characters derived from the aperture measurements of autozooids and measurements of zooids distal to ovicells, while taxonomically significant, were not included in our character matrix because monographs typically report opesia measurements instead of aperture measurements for autozooids, and few specify measurements of autozooids distal to ovicells.

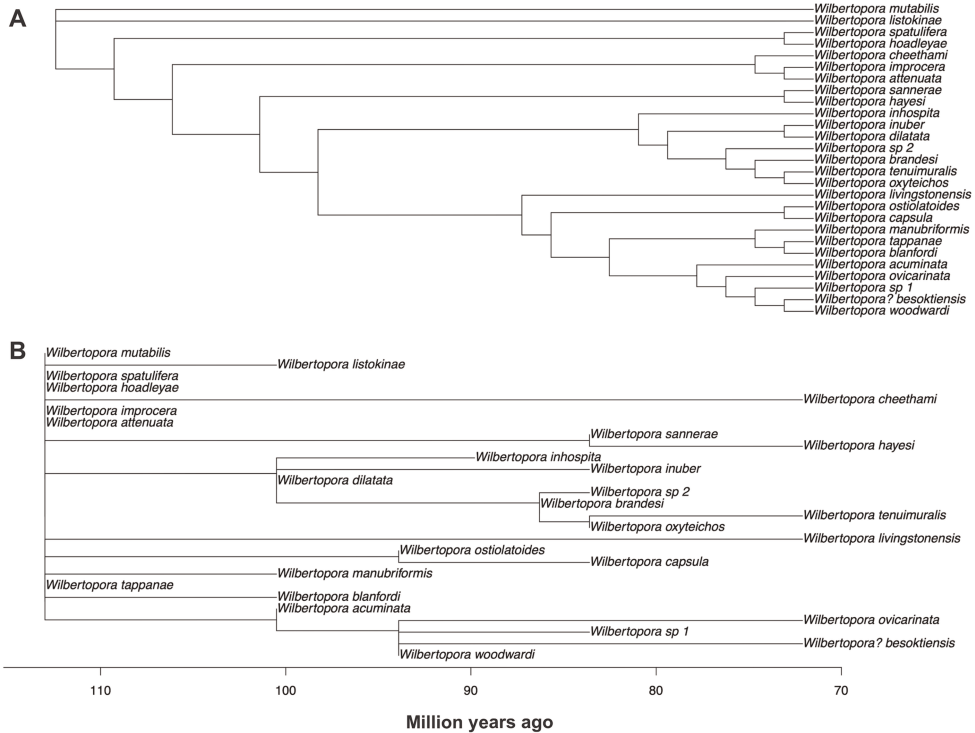


Figure 3. Phylogenetic trees used in this study. A, maximum parsimony tree for *Wilbertopora* completed in PAUP* (Swofford 2003). B, maximum-likelihood tip-dated phylogeny generated using Paleotree (Bapst 2012). Tip dates clump according to geologic stage, with species lineages terminating at the start of the geologic stage of their extinction. Note: due to the small size of our character matrix, the topology of this phylogeny contains several polytomies. We primarily used this phylogeny for the estimation of species richness over time.

Thus, we use phylogenetic studies on other groups of animals that identify novel and phylogenetically significant characters, like shape ratios of features and presence/absence of certain ecologically significant characters (Atteberry & Eberle 2021; Cole 2019), as guides for developing an additional five characters (11, 15, 16, 19, 20 in our character matrix, Table 1). Since zooid shape characteristics and colony-level characters (e.g., the ratio of autozooid opesia to autozooid length, or the presence/absence of spines, respectively) both contain information about the soft tissue features or potential ecological adaptations of zooids and colony ecology, we use these features as additional characters in our character matrix.

Using our character matrix, we generated a set of 10 maximum parsimony phylogenetic trees using a heuristic search over 10,000 iterations in PAUP* (Swofford 2003) and selected the one with the fewest polytomies for tip dating (Figure 3A). Then, using the package Paleotree in Rstudio (Bapst 2012), we used the first and last appearances of each species to generate a maximum-likelihood tip-dated phylogeny (Figure 3B). The purpose of this phylogeny was to supplement our

occurrence information due to the low species sampling during the Santonian and Coniacian stages. The small number of characters in the character matrix led to the generation of several polytomies in our phylogeny, but since this phylogeny is for the purpose of diversity estimation and not topology analysis, we accept this preliminary phylogeny as a measure of species diversity over the course of the Cretaceous.

2.3 Estimating disparity

There are two fundamental ways in which morphologies can vary: shape and size. To get an accurate estimate of size disparity in *Wilbertopora*, we use species mean linear measurements either taken from monographs or from mean values from available SEM images in museum databases. The characters we use for our size estimates of disparity are autozooid length, autozooid width, avicularium length, and avicularium width. While these size metrics do pertain to the functional biology of bryozoans, zooid size may also be influenced by temperature and seasonality (O'Dea & Okamura 1999; Okamura 1992). However, since climate

Table 1. Character matrix for *Wilbertopora* phylogeny. Enumerated characters and their corresponding state values are specified in Appendix 1.

Species	Characters																			
	1	2	3	4	5	6	7	8	9	10	11	12	13	14	15	16	17	18	19	20
<i>W. acuminata</i>	3	0	0	0	1	0	1	1	1	1	1	2	4	2	0	0	1	1	3	3
<i>W. attenuata</i>	2	1	1	0	2	1	0	0	1	1	0	2	4	2	1	0	3	1	3	2
<i>W. blanfordi</i>	5	1	0	0	1	2	1	1	1	1	0	0	1	2	0	1	2	2	4	5
<i>W. brandesi</i>	1	4	1	1	4	4	1	0	0	1	0	1	5	3	1	2	5	4	3	3
<i>W. capsula</i>	4	3	2	2	1	2	2	1	1	1	1	0	0	2	3	2	0	2	3	2
<i>W. cheethami</i>	2	3	1	0	0	0	0	0	1	1	0	1	1	2	1	1	0	0	3	2
<i>W. dilatata</i>	3	4	0	0	4	4	0	1	0	1	0	0	5	1	0	1	5	4	3	1
<i>W. hayesi</i>	2	0	1	0	2	1	0	1	1	1	1	2	3	1	3	2	3	0	4	5
<i>W. headleyae</i>	1	1	1	0	0	1	1	1	1	1	0	2	1	2	1	1	0	0	3	3
<i>W. improcera</i>	2	1	1	0	1	1	0	0	1	1	1	2	2	2	1	2	2	1	3	2
<i>W. inhospita</i>	6	4	1	1	4	4	0	1	0	1	0	0	5	0	1	1	5	4	2	2
<i>W. inuber</i>	2	4	3	1	4	4	0	2	0	1	0	2	5	0	0	0	5	4	0	0
<i>W. listokinae</i>	0	2	1	0	2	2	1	1	1	1	1	2	1	3	1	1	3	3	3	1
<i>W. livingstonensis</i>	5	1	1	1	2	2	0	1	1	1	1	0	1	2	1	1	2	1	3	1
<i>W. manubriformis</i>	4	1	0	0	1	2	1	1	1	1	1	0	1	2	0	0	2	1	3	2
<i>W. mutabilis</i>	2	2	1	0	2	2	1	1	1	1	0	2	1	2	1	1	2	3	3	1
<i>W. ostiolatoides</i>	3	3	1	1	0	1	1	1	1	1	1	0	0	1	1	2	0	0	2	3
<i>W. ovicarinata</i>	3	1	0	0	1	1	0	0	1	1	1	1	0	0	0	1	1	2	2	2
<i>W. oxyteichos</i>	1	4	2	2	4	4	1	2	0	1	0	0	5	1	4	3	5	4	4	3
<i>W. sannerae</i>	0	0	1	0	2	1	0	1	1	1	0	2	4	1	1	1	1	1	2	2
<i>W. sp 1</i>	6	1	0	0	0	0	4	4	1	0	0	1	2	4	0	0	0	0	2	2
<i>W. sp 2</i>	4	4	1	1	4	4	3	2	0	1	0	0	5	2	2	2	5	4	3	2
<i>W. spatulifera</i>	1	1	1	0	2	1	1	1	1	1	0	3	3	2	1	1	3	2	3	2
<i>W. tappanae</i>	2	2	0	0	1	2	1	0	1	1	1	0	1	3	0	0	2	3	2	1
<i>W. tenuimuralis</i>	0	4	1	1	4	4	1	1	0	1	0	0	5	1	2	2	5	4	3	3
<i>W. woodwardi</i>	5	1	4	3	3	3	2	3	1	1	0	1	2	1	4	4	4	3	3	2
<i>W.? besoktiensis</i>	2	1	3	2	3	2	3	3	1	1	0	1	2	1	2	2	1	1	2	1

zones of the Cretaceous were relatively stable at mid-latitudes (Hay & Floegl 2012), and *Wilbertopora* is primarily found in mid-latitudinal regions (excepting *W. tenuimuralis* (Di Martino *et al.* 2018)), the impact of temperature and seasonality on the differences in zooid sizes across species is likely minimal.

To get an estimate of shape disparity, we used Elliptical Fourier Analysis (EFA) to quantify autozooid and avicularium operculum shape (Crampton 1995). We chose to measure the outlines of opercula because that is the portion of the zooid exoskeleton most divergent between autozooids and avicularia (Carter 2008; Kauffman 1971). The divergence in opercular shape corresponds to the different functionalities of autozooids and avicularia, as the operculum indirectly reflects polypide morphology. We used Fiji (Schindelin *et al.* 2012) to manually collect outlines of the opercula of autozooids and avicularia in all 25 species. On each measured zooid, we marked the starting measurement point as the most distal end of the zooid operculum and captured outlines in a clockwise fashion. We collected operculum outlines of two zooids belonging to each zooid type in each species and averaged their EFA coefficients to get an estimate of shape disparity of autozooids and avicularia for each species. We ran a principal components analysis of the EFA coefficients across all species and took resulting first principal components of autozooids and avicularia as our shape metrics.

To calculate disparity using these values, we calculated centroid size for each geologic stage from

the Albian to the Maastrichtian (Foote 1993). We computed centroid size by taking species means for each character, and then summing the square distances of each species mean from the pooled mean for each geologic stage. We scaled these summed square distances by the number of species in each geologic stage, so that stages with different levels of species richness could be directly compared.

We computed three disparity measures for each geologic stage: total disparity, avicularian disparity, and autozooidal disparity. We can therefore assess how each zooid type contributes to the signature of total disparity across each geologic stage and assess whether different zooid types have different evolutionary trajectories as *Wilbertopora* diversifies.

3 RESULTS AND DISCUSSION

3.1 Disparity and diversity over time

Our results show that disparity and diversity are largely decoupled (Figure 4). Disparity increases monotonically from the Albian (beginning 113 Ma) to the Turonian (ending 89.6 Ma), where it reaches an absolute maximum. For the rest of the Cretaceous, disparity declines monotonically.

The diversity curve of *Wilbertopora* follows a different pattern from disparity (Figure 4). Taxonomic diversity begins at a local maximum in the Albian, and then it alternates between local maxima and local minima until it reaches an absolute peak in the Campanian (beginning 83.6

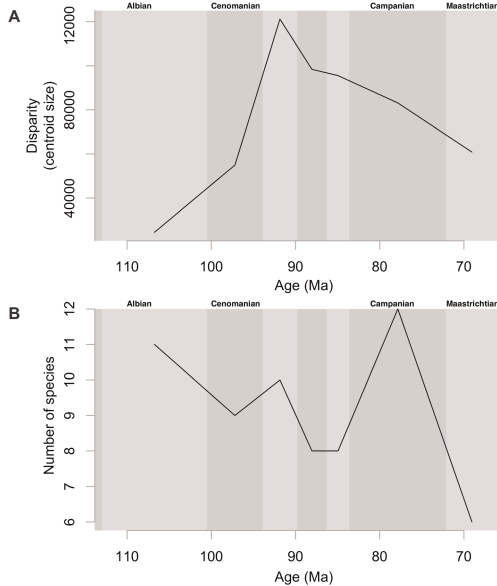


Figure 4. Disparity (A) and diversity (B) of *Wilbertopora*. Disparity reaches a single peak during the Turonian (93.9 Ma – 89.8 Ma), whereas diversity exhibits a more varied trajectory.

Ma). The Maastrichtian sees the largest drop in taxonomic diversity in the Cretaceous, with species richness dropping from 12 to 6 species.

3.2 Diversity-disparity analysis

Directly comparing diversity and total disparity using Jablonski's (2017) diversity-disparity analysis shows the extent of the decoupled nature of disparity and diversity during *Wilbertopora*'s genus lifespan (Figure 5A). Comparing *Wilbertopora*'s pattern of diversity and disparity with the three types of diversification trajectories explicated by Jablonski (2017) reveals surprising results. The diversity-disparity patterns of *Wilbertopora* have an unusual signature: the changes in diversity and disparity do not follow a single trajectory. Instead, the genus appears, across all levels of analysis (Figure 5), to begin its diversification according to ecological exploitation, then shifting into ecological exploration in most of the latter half of its stratigraphic range. Most of the genus's diversification occurs above the 1:1 line, indicating that different species of *Wilbertopora* are exhibiting disparate zooid morphologies.

3.3 Avicularian versus autozooidal disparity

Comparison of the avicularian and autozooidal diversity-disparity analyses shows that the two body types generally follow the same trajectory shape (Figure 5 B-C). However, diversity-disparity plots are scaled by value ranges, and are not suitable for direct comparisons of

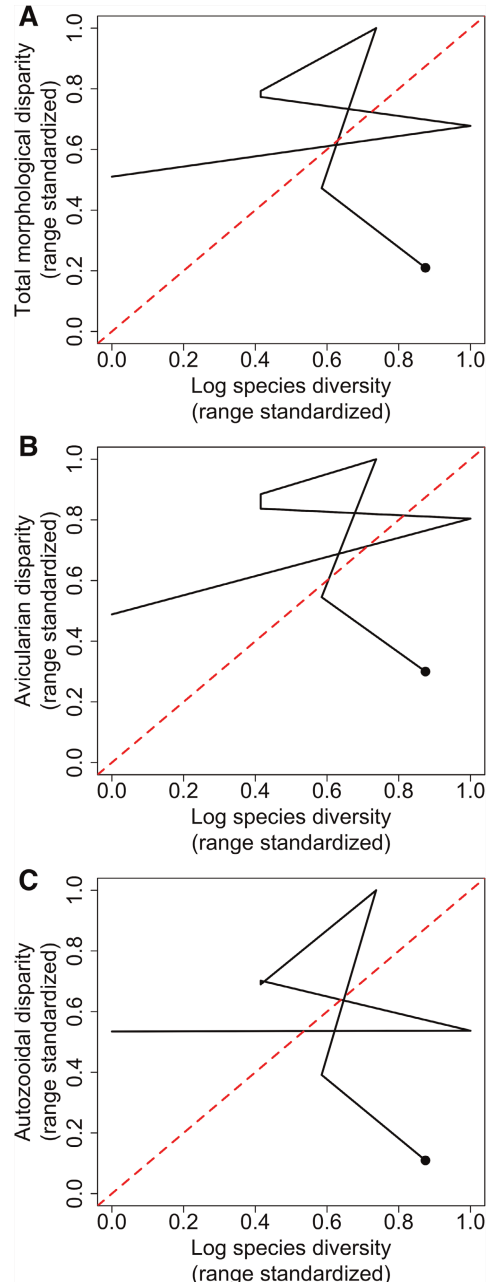


Figure 5. Disparity-disparity plots of *Wilbertopora*. A, total morphologic disparity versus species diversity of *Wilbertopora* over the genus' life span. B, disparity of avicularian characters in *Wilbertopora* versus diversity over the genus life span. C, autozooidal disparity of *Wilbertopora* versus diversity over the genus' life span. In all panels, the dashed red line shows a line with a slope of 1, which is the expected pattern in a diversification event where disparity and the log of diversity increase proportionately (i.e., Jablonski's (2017) Type 2). These plots show time series, beginning with the circle in the bottom right portion of each graph. Each subsequent change in slope corresponds to the onset of a new geologic stage.

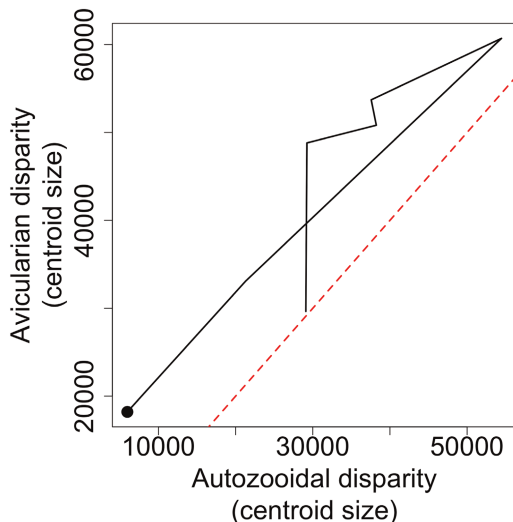


Figure 6. Plot of avicularian disparity versus autozooidal disparity. This represents a time series going from the Albian (circle) to the Maastrichtian (line ends). The raw values of disparity of each zooid type are directly compared to assess how their relationship changes over the course of *Wilbertopora* diversification. Dashed red line (i.e., slope = 1) indicates Jablonski's (2017) Type 2 event.

different disparity measures. Comparing raw avicularian disparity values and raw autozooidal disparity values directly is a more direct comparison of the two measures (Figure 6). For *Wilbertopora*'s genus life span, avicularia have a higher disparity during each geologic stage than autozooids. This result indicates that avicularia contribute more heavily to the signature of “ecological exploration” that *Wilbertopora* exhibits during its diversification than autozooids.

Overall, our results indicate that both avicularia and autozooids experienced increases in disparity relative to diversity as *Wilbertopora* diversified. *Wilbertopora* may have experienced selective pressure to generate autozooids of differing sizes during this time, as a response to substrate competition. Encrusting bryozoans must maximize occupation of substrate space to ensure survival, and many modern bryozoans exhibit wide ranges of autozooid shapes and sizes (McKinney & Jackson 1991). Perhaps expansion of autozooidal phenotypes in *Wilbertopora* is evidence of this selective pressure guiding the genus's diversification.

Avicularia show the strongest pattern of ecological exploration during *Wilbertopora* diversification. The divergent morphology of avicularia is not unique to *Wilbertopora*. Avicularia in extant taxa have a variety of functions, including colony defense, hygiene, and the maintenance of feeding currents

(Kaufmann 1971; McKinney & Jackson 1991; Winston 1986). The divergent morphologies of the early avicularia in *Wilbertopora* suggest that avicularia may have evolved to serve a variety of functions from its origination. Since there is no conserved morphological form for avicularia, even among the closely related members of this single genus, there is likely a range of avicularian function for each lineage of *Wilbertopora*. This suggests that from the first appearance of avicularia, their functional morphology has been widely divergent, even among different species of the same genus.

4 FUTURE CONSIDERATIONS

Since this study is preliminary by nature, there is a limit to the conclusions that can be drawn from these results. A lineage-specific analysis of *Wilbertopora* avicularian evolution is a natural next step but requires a resolved phylogeny of the genus. To make this possible, a much larger character matrix (with 100+ characters) is required. Furthermore, analysis of partial disparity of *Wilbertopora* species using whole-colony specimens would reveal whether there are species-level constraints on avicularian morphology in *Wilbertopora*, or whether each species can express a large range of avicularian morphology.

ACKNOWLEDGEMENTS

We would like to thank the Natural History Museum in London and the National Museum of Natural History in Washington, D.C. for making SEMs of their bryozoan specimens accessible via their online databases. This research was supported by the Bruce and Marcy Benson Graduate Student Fellowship in the Department of Geological Sciences at the University of Colorado, Boulder.

REFERENCES

- Atteberry, M.R. & Eberle, J.J. 2021. New Earliest Paleocene (Puercan) Periptychid ‘Condylarths’ from the Great Divide Basin, Wyoming, USA. *Journal of Systematic Palaeontology* 19(8): 565–593.
- Bapst, D.W. 2012. Paleotree: An R Package for Paleontological and Phylogenetic Analyses of Evolution. *Methods in Ecology and Evolution* 3: 803–807.
- Bock, P. 2020. *Recent and Fossil Bryozoa*. The Bryozoa Home Page. Retrieved August 14, 2022, from <http://bryozoa.net/>.
- Carter, M.C. 2008. *The Functional Morphology of Avicularia in Cheilostome Bryozoans*. Ph.D. thesis. Victoria University of Wellington, 223 p.
- Cheetham, A.H. 1954. A New Early Cretaceous Cheilostome Bryozoan from Texas. *Journal of Paleontology* 28(2): 177–184.

- Cheetham, A.H., Sanner, J., Taylor, P.D. & Ostrovsky, A.N. 2006. Morphological Differentiation of Avicularia and the Proliferation of Species in Mid-Cretaceous *Wilbertopora* Cheetham, 1954 (Bryozoa: Cheilostomata). *Journal of Paleontology* 80(1): 49–71.
- Cole, S.R. 2019. Phylogeny and Evolutionary History of Diplobathrid Crinoids (Echinodermata). *Palaeontology* 62(3): 357–373.
- Crampton, J.S. 1995. Elliptic Fourier Shape Analysis of Fossil Bivalves: Some Practical Considerations. *Lethaia* 28(2): 179–186.
- Di Martino, E. & Taylor, P.D. 2013. First Bryozoan Fauna from a Tropical Cretaceous Carbonate: Simsima Formation, United Arab Emirates–Oman Border Region. *Cretaceous Research* 43: 80–96.
- Di Martino, E., Martha, S.O. & Taylor, P.D. 2018. The Madagascan Maastrichtian bryozoans of Ferdinand Canu – Systematic Revision and Scanning Electron Microscopic Study. *Annales de Paléontologie* 104(2): 101–128.
- Foote, M. 1993. Contributions of Individual Taxa to Overall Morphological Disparity. *Paleobiology* 19(4): 403–419.
- Guha, A.K. 1989. Upper Cretaceous Cheilostomes (Bryozoa) from the Bagh Sediments of Madhya Pradesh. In P. Kalia (ed), *Micropalaeontology of the Shelf Sequences of India*: 118–131. New Delhi: Papyrus Publishing House.
- Hay, W.W. & Floegel, S. 2012. New Thoughts About the Cretaceous Climate and Oceans. *Earth Science Reviews* 115(4): 262–272.
- Jablonski, D. 2017. Approaches to Macroevolution: 2. Sorting of Variation, Some Overarching Issues, and General Conclusions. *Evolutionary Biology* 44(4): 451–475.
- Jablonski, D., Lidgard, S. & Taylor, P.D. 1997. Comparative Ecology of Bryozoan Radiations; Origin of Novelties in Cyclostomes and Cheilostomes. *PALAIOS* 12(6): 505–523.
- Kaufmann, K.W. 1971. *The Form and Functions of the Avicularia of Bugula [phylum Ectoprocta]*. New Haven: Peabody Museum of Natural History.
- Koromylova, A.V., Baraboshkin, E.Y. & Martha, S.O. 2018. Late Campanian to Late Maastrichtian Bryozoans Encrusting on Belemnite Rostra from the Aktolagay Plateau in Western Kazakhstan. *Geobios* 51(4): 307–333.
- Martha, S.O. & Taylor, P.D. 2016. A New Western European Cretaceous Bryozoan Genus from the Early Cenomanian Radiation of Neocheilostomes. *Papers in Palaeontology* 2(2): 311–321.
- McKinney, F.K. & Jackson, J.B.C. 1991. *Bryozoan Evolution*. Chicago: University of Chicago Press.
- O'Dea, A. & Okamura, B. 1999. Influence of Seasonal Variation in Temperature, Salinity and Food Availability on Module Size and Colony Growth of the Estuarine Bryozoan *Conopeum seurati*. *Marine Biology*, 135(4): 581–588.
- Okamura, B. 1992. Microhabitat Variation and Patterns of Colony Growth and Feeding in a Marine Bryozoan. *Ecology*, 73(4): 1502–1513.
- Ostrovsky, A.N., Taylor, P.D., Dick, M.H. & Mawatari, S. F. 2008. Pre-Cenomanian Cheilostome Bryozoa: Current State of Knowledge. In H. Okada, S.F. Mawatari, N. Suzuki & P. Gautam (eds), *Origin and Evolution of Natural Diversity: Proceedings of the International Symposium, The Origin and Evolution of Natural Diversity, held from 1–5 October 2007 in Sapporo, Japan*: 69–74. Sapporo: Hokkaido University.
- Schindelin, J., Arganda-Carreras, I., Frise, E. et al. 2012. Fiji: An Open-source Platform for Biological-image Analysis. *Nature Methods* 9(7): 676–682.
- Smith, A.B. & Batten, D.J. 2002. *Fossils of the Chalk*. London: Palaeontological Association.
- Swofford, D.L. 2003. *PAUP*. Phylogenetic Analysis Using Parsimony (*and Other Methods)*. Version 4. Sunderland, Massachusetts: Sinauer Associates.
- Taylor, P.D. & Badve, R.M. 1994. The Mid-Cretaceous Bryozoan Fauna from the Bagh Beds of Central India: Composition and Evolutionary Significance. In P.J. Hayward, J.S. Ryland & P.D. Taylor (eds), *Biology and Palaeobiology of Bryozoans*: 181–186. Fredensborg: Olsen & Olsen.
- Taylor, P.D. & Martha, S.O. 2017. Cenomanian Cheilostome Bryozoans from Devon, England. *Annales de Paléontologie* 103(1): 19–31.
- Taylor, P.D. & McKinney, F.K. 2006. Cretaceous Bryozoa from the Campanian and Maastrichtian of the Atlantic and Gulf coastal plains, United States. *Scripta Geologica* 132: 1–346.
- Taylor, P.D. 1988. Major Radiation of Cheilostome Bryozoans: Triggered by the Evolution of a New Larval Type? *Historical Biology* 1(1): 45–64.
- Taylor, P.D. 2008. Late Cretaceous Cheilostome Bryozoans from California and Baja California. *Journal of Paleontology* 82(4): 823–834.
- Taylor, P.D. 2020. *Bryozoan Paleobiology*. Hoboken, NJ: Wiley.
- Voigt, E. 1981. Répartition et Utilisation Stratigraphique des Bryozoaires du Crétacé Moyen (Aptien-Coniacien). *Cretaceous Research* 2(3): 439–462.
- Winston, J.E. 1986. Victims of Avicularia. *Marine Ecology* 7(2): 193–199.
- Zitt, J., Vodrážka, R., Hradecká, L., Svobodová, M. & Zágoršek, K. 2006. Late Cretaceous Environments and Communities as Recorded at Chřnky (Bohemian Cretaceous Basin, Czech Republic). *Bulletin of Geosciences* 81(1): 43–79.

APPENDIX 1

Characters are coded as follows:

- 1: first principal component (PC1) of outline of autozooid operculum. 0 = -0.051 to 0; 1 = 0.001 to 0.050; 2 = 0.051 to 0.100; 3 = 0.101 to 0.150; 4 = 0.151 to 0.200; 5 = 0.201 to 0.250; 6 = 0.251 to 0.300.
- 2: PC1 of outline of avicularium operculum. 0 = -0.49 to -0.30; 1 = -0.29 to -0.10; 2 = -0.09 to 0.10; 3 = 0.11 to 0.30; 4 = N/A.
- 3: autozooid length. 0 = 301 to 450 µm; 1 = 451 to 600 µm; 2 = 601 to 750 µm; 3 = 751 to 900 µm; 4 = 901 to 1050 µm.
- 4: autozooid width. 0 = 201 to 350 µm; 1 = 351 to 500 µm; 2 = 501 to 650 µm; 3 = 651 to 800 µm; 4 = N/A.
- 5: avicularium length. 0 = 201 to 350 µm; 1 = 351 to 500 µm; 2 = 501 to 650 µm; 3 = 651 to 800; 4 = N/A.
- 6: avicularium width. 0 = 51 to 150 µm; 1 = 151 to 250 µm; 2 = 251 to 350 µm; 3 = 351 to 450 µm; 4 = N/A.

- 7: ovicell length. 0 = 101 to 150 μm ; 1 = 151 to 200 μm ; 2 = 201 to 250 μm ; 3 = 251 to 300 μm ; 4 = N/A.
- 8: ovicell width. 0 = 101 to 170 μm ; 1 = 171 to 240 μm ; 2 = 241 to 310 μm ; 3 = 311 to 380 μm ; 4 = N/A.
- 9: presence/absence of avicularia. 0 = absent; 1 = present.
- 10: presence/absence of ovicells. 0 = absent; 1 = present.
- 11: presence/absence of spines. 0 = absent; 1 = present.
- 12: autozooid length / autozooid width ratio. 0 = 1.21 to 1.40; 1 = 1.41 to 1.60; 2 = 1.61 to 1.80; 3 = 1.81 to 2.00; 4 = N/A.
- 13: avicularia length / avicularia width ratio. 0 = 1.01 to 1.50; 1 = 1.51 to 1.90; 2 = 1.91 to 2.30; 3 = 2.31 to 2.70; 4 = 2.71 to 3.10; 5 = N/A.
- 14: ovicell length / ovicell width ratio. 0 = 0.501 to 0.650; 1 = 0.651 to 0.800; 2 = 0.801 to 0.950; 3 = 0.951 to 1.100; 4 = N/A.
- 15: autozooid opesia length. 0 = 191 to 290 μm ; 1 = 291 to 390 μm ; 2 = 391 to 490 μm ; 3 = 491 to 590 μm ; 4 = 591 to 690 μm .
- 16: autozooid opesia width. 0 = 101 to 180 μm ; 1 = 181 to 260 μm ; 2 = 261 to 340 μm ; 3 = 341 to 420 μm ; 4 = 421 to 500 μm .
- 17: avicularium aperture length. 0 = 81 to 200 μm ; 1 = 201 to 320 μm ; 2 = 321 to 440 μm ; 3 = 441 to 560 μm ; 4 = 561 to 680 μm .
- 18: avicularium aperture width. 0 = 51 to 100 μm ; 1 = 101 to 150 μm ; 2 = 151 to 200 μm ; 3 = 201–250 μm ; 4 = N/A.
- 19: autozooid opesia length / autozooid length ratio. 0 = 0.201 to 0.350; 1 = 0.351 to 0.500; 2 = 0.501 to 0.650; 3 = 0.651 to 0.800; 4 = 0.801 to 0.950.
- 20: autozooid opesia width / autozooid width ratio. 0 = <0.51; 1 = 0.51 to 0.60; 2 = 0.61 to 0.70; 3 = 0.71 to 0.80; 4 = 0.81 to 0.90, 5 = 0.91 to 1.00.